A&A 374, 919–931 (2001)
DOI: 10.1051/0004-6361:20010831

Astronomy & Astrophysics

Global emission line trends in spiral galaxies: The reddening and metallicity sequences

G. Stasińska[1] and L. Sodré Jr.[2]

[1] DAEC, Observatoire de Paris-Meudon, 92195 Meudon Cedex, France
e-mail: grazyna.stasinska@obspm.fr
[2] Departamento de Astronomia, Instituto Astronômico e Geofísico da USP, Av. Miguel Stefano 4200, 04301-904 São Paulo, Brazil
e-mail: laerte@iagusp.usp.br

Received 21 February 2001 / Accepted 5 June 2001

Abstract. We have explored the emission line trends in the integrated spectra of normal spiral galaxies of the Nearby Field Galaxy Survey (Jansen et al. 2000a, b), in order to investigate the relationships between dust extinction, metallicity and some macroscopic properties of spiral galaxies. We found a very strong correlation between the Hβ and Hα equivalent widths, implying that the difference between the extinction of the stellar and the nebular light depends only on the intrinsic colours of the galaxies, being larger for redder galaxies. The usual metallicity indicator for giant H II regions ([O III] λ4959,5007 + [O II] λ3726,3729)/Hβ is not appropriate for integrated spectra of spiral galaxies, probably due to metallicity gradients. Much better qualitative metallicity indicators are found to be [N II] λ6584/[O II] λ3726,3729 and [N II] λ6584/Hα, the latter having the advantage of being independent of reddening and being applicable also for galaxies with weak emission lines. With these indicators, we find that the nebular extinction as derived from the Balmer decrement strongly correlates with the effective metallicity of the emission line regions. The overall metallicity of the emission line regions is much better correlated with galaxy colours than with morphological types. A Principal Component Analysis on a 7-D parameter space showed that the variance is produced, in first place, by the metallicity and parameters linked to the stellar populations, and, in second place, by the surface brightness, which is linked to the dynamical history of the galaxies. The absolute magnitude, related to the mass of the galaxy, comes only in third place.

Key words. galaxies: spirals – galaxies: abundances – galaxies: evolution – galaxies: ISM – galaxies: stellar content

1. Introduction

The interpretation of integrated spectra of nearby galaxies becomes increasingly important with the profusion of studies of galaxies in clusters (e.g., Caldwell et al. 1993; Dressler et al. 1999; Poggianti et al. 1999; Balogh et al. 1999) and galaxies at large redshifts (e.g., Colless et al. 1990; Hammer et al. 1997; Lilly et al. 1998; Guzman et al. 1998).

Indeed, for the studies of distant galaxies, the spatial resolution obtained with ground-based instruments makes any morphological classification difficult, and even from space, morphological studies are bound to be crude. Therefore, most information on distant galaxies will come from photometry or spectroscopy, and the sampled regions will cover a significant part – if not all – of the galaxy surface.

Send offprint requests to: G. Stasińska,
e-mail: grazyna.stasinska@obspm.fr

Techniques have been devised to classify galaxies using their spectra only (Morgan & Mayall 1957; Sodré & Cuevas 1994, 1997; Connolly et al. 1995; Zaritsky et al. 1994; Folkes et al. 1996; Galaz & de Lapparent 1998; Sodré & Stasińska 1999). It has been shown that the results correlate rather well with the galaxy morphological types. The spectral classification actually presents some advantages even for the study of nearby galaxies: whatever criteria are adopted, they allow an objective and continuous classification of the galaxies, in contrast with the conventional morphological classification which is by nature subjective and provides discrete classes. In addition, any interpretation in terms of stellar content and evolution is directly related with the galaxy spectra, while the link with galaxy morphology is rather elusive.

In a former paper (Sodré & Stasińska 1999, hereinafter SS99), based on the integrated spectra for normal spiral galaxies from the Kennicutt (1992) atlas, we have shown that emission line ratios and equivalent widths are impressively well correlated with the galaxy spectral type

obtained from a Principal Component Analysis of the continuum and the absorption features. The correlation is far better with galaxy spectral types than with morphological types. We also found that the extinction derived from the emission line Balmer decrement correlates with the galaxy spectral type, being larger for early type galaxies.

But the sample was small: there were only 15 *normal* spirals in the Kennicutt (1992) atlas. In the meantime, Jansen et al. (2000a and 2000b) published a comprehensive photometric and spectrophotometric atlas of 200 nearby field galaxies (the Nearby Field Galaxy Survey, hereinafter NFGS). The objects were selected so as to span the full range in galaxy luminosities and morphological types. As in Kennicutt (1992), the integrated galaxy spectra were obtained by drifting a long slit across the galaxy. This considerably richer and more appropriate database motivated us to revisit the study of SS99, in order to see whether the formerly found trends are confirmed, and to refine their empirical interpretation.

In this paper, we investigate the overall effective extinction and metallicity of spiral galaxies through an empirical analysis of the properties of their global emission lines. We also perform a Principal Component Analysis in order to understand the relation amongst the variables describing the galaxies.

As in SS99, our paper deals only with normal galaxies. Therefore, we have rejected from the NFGS sample all the galaxies with Seyfert nuclei and nuclear starbursts, as well as the galaxies with indication of close interaction or strong peculiarity, as indicated in the appendix of Jansen et al. (2000a). In the following, the expression NFGS sample will refer to the 158 galaxies that have no evident sign of peculiarity.

All the galaxies in our sample are found at redshifts lower than 0.05. Their blue absolute magnitudes range between -22 and -13. For most of the diagrams investigated in this paper, relevant data are available for 100–120 objects.

2. Dust extinction

The dust content of galaxies is a controversial subject. While the first comprehensive analysis of this problem (Holmberg 1958, 1975; de Vaucouleurs 1959) have proposed that spiral disks are largely transparent, more recent works have suggested that these disks are opaque or at least far more obscured than previously thought (cf. Valentijn 1990; Disney et al. 1989; James & Puxley 1993). So far, there is still no consensus on whether galaxies are optically thick or thin (see Wang & Heckman 1996 or Meurer & Seibert 2001 and references therein). Actually, the galaxy extinction depends not only on the amount of dust and its composition, but also on the distribution of dust relative to the light sources. This point too has been disputed. For instance, some authors suggest a foreground screen dust geometry (Calzetti et al. 1994, 1996; but see Witt et al. 1992), while others propose hybrid models, with the dust partially distributed in a foreground screen and partially concentrated in the star-forming regions (e.g. Charlot & Fall 2000). Indeed, Charlot & Fall (2000; see also Charlot & Longhetti 2001) present a model for the effects of dust on integrated galaxy spectra that explains several observational properties of starburst galaxies, showing that there is a sequence in the overal dust content of the galaxies. Radial gradients should also play a role, and Giovanelli et al. (1994) and Peletier et al. (1995) propose that the dust distribution presents a strong radial dependence, with considerable obscuration near the centers of galaxies and little at the outer edges (see also Nelson et al. 1998).

In nearby starburst galaxies, there is evidence from bidimensional spectroscopy that stars, gas and dust are decoupled (Maíz-Apellániz et al. 1998) and the attenuation inferred from the Hα/Hβ ratio is typically higher than that inferred from the spectral continuum (e.g., Fanelli et al. 1988; Calzetti et al. 1994; Mayya & Prahbu 1996; Calzetti 1997). Recently, Poggianti et al. (1999) and Poggianti & Wu (2000) have shown that the so-called e(a) spectrum can be reproduced assuming that in a current starburst the dust extinction affects the young stellar populations much more than the older stars. This effect has been called selective dust extinction by Poggianti and collaborators, and is a consequence of the fact that a large fraction – but not all – of the dust in galaxies is associated with star formation regions, absorbing a significant fraction of the light emitted by the young stars. We now present empirical evidence that selective extinction is indeed affecting the integrated spectra of spiral galaxies.

2.1. Selective extinction

Figure 1 shows the emission line equivalent width of Hβ, EW(Hβ), as a function of that of Hα, EW(Hα), for the 110 galaxies from the NFGS sample with available data. The shape of the symbols correspond to different morphological classes, as indicated in the figure caption. As explained by Jansen et al. (2000b), these equivalent widths were extracted from the spectra by placing the limits of the measurement window well inside the absorption trough, thus minimizing the effect of the underlying stellar absorption, which becomes appreciable at small equivalent widths. Following the prescription of Jansen et al. (2001), we have applied an additional correction for residual absorption (1.5 Å for Hα and 1 Å for Hβ).

The correlation between EW(Hβ) and EW(Hα) is impressively strong and is well represented by a relation of the type

$$EW(\mathrm{H}\beta) = A \times EW(\mathrm{H}\alpha) \quad (1)$$

where A is a constant. Using the ordinary least squares bisector estimation for the fitting (Isobe et al. 1990), we find $A = 0.245 \pm 0.007$. This correlation is even better than the one found by SS99 for the Kennicutt sample. The uncertainties in the emission line equivalent widths may be appreciable for EW(Hα) or EW(Hβ) smaller than, say,

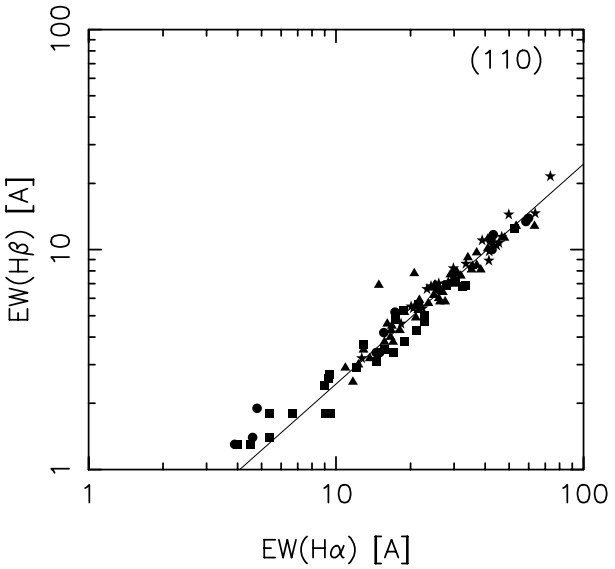

Fig. 1. $EW(\mathrm{H}\beta)$ as a function of $EW(\mathrm{H}\alpha)$ for the normal spiral galaxies from the NFGS sample. Different symbols correspond to galaxies of different morphological types T. Circles: $-5 \leq T \leq 0$; squares: $1 \leq T \leq 3$; triangles: $4 \leq T \leq 6$; Circles: $7 \leq T \leq 10$. The total number of the objects appearing in the diagram is given in parenthesis. Such a presentation is adopted for all the observational diagrams in this paper. The $EW(\mathrm{H}\beta) = 0.245\ EW(\mathrm{H}\alpha)$ line is shown.

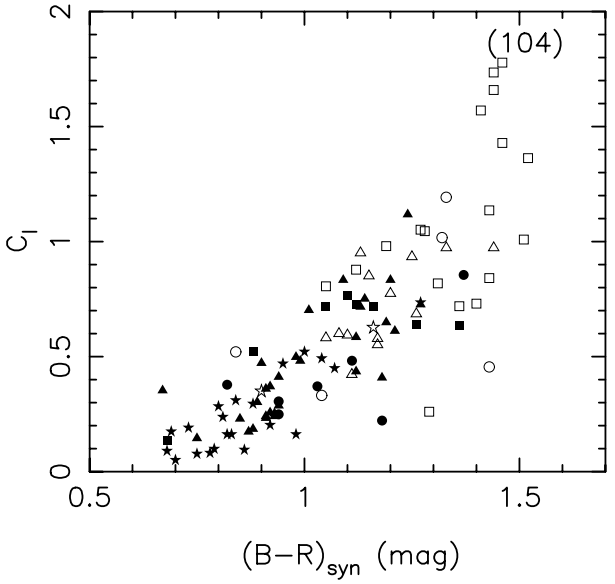

Fig. 2. C_l as a function of the galaxy synthetic colour $(B-R)$ derived from the spectra. Symbols have the same meaning as in Fig. 1. Open symbols correspond to galaxies with $EW(\mathrm{H}\alpha) <$ 10 Å or $EW(\mathrm{H}\beta) < 5$ Å.

10 Å but the value of the slope A is essentially determined by larger equivalent widths and is not sensitive to these uncertainties. We have performed a non-parametric Kendall's τ statistical test (Press et al. 1992) to evaluate quantitatively the quality of the fitting, for the whole sample and for the sub-sample with $EW(\mathrm{H}\alpha) > 5$ Å and $EW(\mathrm{H}\beta) > 10$ Å. The results are presented in Table 1 and reveal that the correlation between $EW(\mathrm{H}\alpha)$ and $EW(\mathrm{H}\beta)$ is indeed highly significant for both samples. For easy consultation, the results of this test for all the observational diagrams investigated in this study have been summarized in Table 1. In this table we present, for each plot and sample, the number of data points, the value of the non parametric correlation coefficient τ, and its two-sided significance level, *prob*. Note that small values for *prob* indicates that the correlation or anti-correlation between the variables is significant.

We found that the residuals in the $EW(\mathrm{H}\beta)$ vs. $EW(\mathrm{H}\alpha)$ relation are independent of the galaxy ellipticity (therefore inclination) as well as of the galaxy absolute magnitude (and any combination of ellipticity and magnitude). They are also independent of galaxy morphological type.

The correlation shown in Fig. 1 has important implications concerning the nature of the internal reddening of the galaxies, in particular in terms of a link between the effective extinction in the continuum and in the emission lines. Let us write an emission line equivalent width as a ratio between the emission line intensity I and the flux F_c at the adjacent continuum in the observed spectrum: $EW = I/F_\mathrm{c}$. The relation between the observed and intrinsic (i.e., extinction corrected) intensities of Hα and Hβ is

$$\frac{I(\mathrm{H}\alpha)}{I(\mathrm{H}\beta)} = \delta \times 10^{-C_\mathrm{l}(f(\mathrm{H}\alpha)-f(\mathrm{H}\beta))} \tag{2}$$

where δ is the intrinsic intensity ratio of these two lines, C_l is a measure of the effective extinction at Hβ in the region producing the lines, and $f(\lambda)$ is a function that gives the wavelength dependence of the extinction. Let C_c be a measure of the effective amount of extinction at the wavelength of Hβ in the region producing the continuum, so that the observed and intrinsic fluxes (denoted by F_c and F_c^0, respectively) at a given wavelength are related by

$$F_\mathrm{c}(\lambda) = F_\mathrm{c}^0(\lambda) \times 10^{-C_\mathrm{c} f(\lambda)}. \tag{3}$$

Equation (1) implies that the effective extinction at Hβ is related to the ratio of the observed continuum fluxes at Hα and Hβ by

$$C_\mathrm{l} = \frac{-1}{f(\mathrm{H}\alpha) - f(\mathrm{H}\beta)} \log\left(\frac{1}{A\delta}\frac{F_\mathrm{c}(\mathrm{H}\alpha)}{F_\mathrm{c}(\mathrm{H}\beta)}\right) \tag{4}$$

and that the difference between the line and continuum effective extinctions is related to the ratio of the intrinsic continuum fluxes by

$$C_\mathrm{l} - C_\mathrm{c} = \frac{-1}{f(\mathrm{H}\alpha) - f(\mathrm{H}\beta)} \log\left(\frac{1}{A\delta}\frac{F_\mathrm{c}^0(\mathrm{H}\alpha)}{F_\mathrm{c}^0(\mathrm{H}\beta)}\right). \tag{5}$$

Since $F_\mathrm{c}^0(\mathrm{H}\alpha)/F_\mathrm{c}^0(\mathrm{H}\beta)$ depends only on the stellar populations of the galaxy, Eq. (5) is indeed an empirical prescription for the relation between selective dust extinction and the galaxy stellar populations.

Although we have no way to determine the value of C_c from the available data, some implications of Eq. (5)

may be inferred. First, the difference between $C_{\rm l}$ and $C_{\rm c}$ is essentially dependent on the intrinsic colour of the galaxy and is larger for intrinsically redder galaxies. Second, if $C_{\rm l} \geq C_{\rm c}$, a lower limit for the intrinsic continuum flux ratio at the wavelengths of Hα and Hβ is $F_{\rm c}^0({\rm H}\alpha)/F_{\rm c}^0({\rm H}\beta) = A\delta$. Assuming $\delta = 2.9$ (the case B recombination value corresponding to a temperature of 9000 K), and using the Seaton (1979) extinction law, we find that $F_{\rm c}^0({\rm H}\alpha)/F_{\rm c}^0({\rm H}\beta)$ in spiral galaxies should be larger than 0.70.

We have used the software PÉGASE.2 (Fioc & Rocca-Volmerange 1997) with a Salpeter IMF and default values to compute this ratio for a few simple model galaxy spectra. For an instantaneous burst 15 Gyr old we obtain $F_{\rm c}^0({\rm H}\alpha)/F_{\rm c}^0({\rm H}\beta) = 0.84$ and Eq. (5) implies $C_{\rm l} - C_{\rm c} = 0.21$, whereas for a model with constant star formation rate and same age this ratio is 0.75 and Eq. (5) leads to $C_{\rm l} - C_{\rm c} = 0.07$. Additional clues about $C_{\rm c}$ may be obtained from spectral synthesis methods that include explicitly in the analysis the effects of extinction on the spectra (e.g., Cid Fernandes et al. 2001).

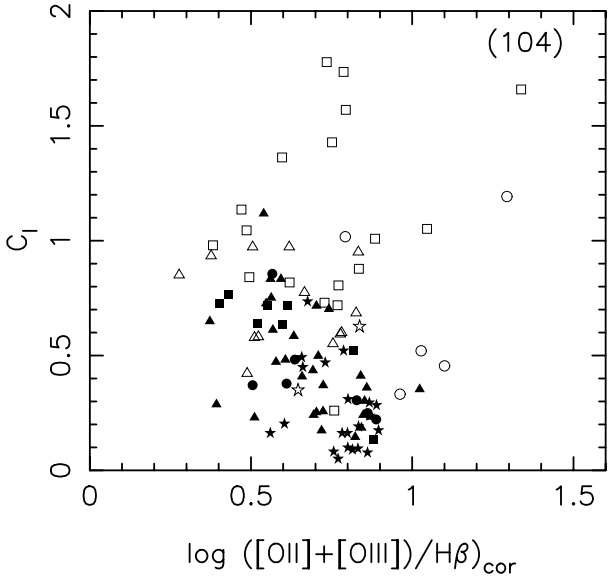

Fig. 3. $C_{\rm l}$ as a function of [O III] λ5007, 4959 + [O II] λ3726, 3729)/Hβ corrected for reddening. Same symbols as in Fig. 2.

2.2. The extinction of the nebular light

We obtained $C_{\rm l}$ from the observed Hα/Hβ ratio for the 110 normal galaxies of the NFGS sample with available data.

Figure 2 plots $C_{\rm l}$ as a function of the galaxy color $(B-R)$. The open symbols correspond to galaxies with $EW({\rm H}\alpha) < 10$ Å or $EW({\rm H}\beta) < 5$ Å for which the value of $C_{\rm l}$ tends to be more uncertain. A very good correlation is seen, with $C_{\rm l}$ larger for redder objects (the correlation coefficient τ shown in Table 1 is larger than 0.6). This behavior is indeed expected from Eq. (4). As already shown by Jansen et al. (2000), there is a correlation between $C_{\rm l}$ and the galaxy blue absolute magnitude, although the dispersion is much larger than for the color. $C_{\rm l}$ also correlates with the morphological types, decreasing towards later types, confirming the trend found in SS99. The maximum extinction is observed for galaxies Sb, but the variance is large. On the other hand, there is no correlation whatsoever with the galaxy apparent ellipticity, implying that at least part of the obscuring dust is concentrated close to the emitting sources.

We now examine whether there is a relation between $C_{\rm l}$ and the overall metallicity of the galaxies. So far, there have been contradictory claims in this respect. Zaritsky et al. (1994) found no evidence for a systematic dependence between reddening and abundance in a sample of 39 disk galaxies. In their study, the characteristic metallicity of the galaxies was derived from the value of the metallicity indicator ([O III] λ5007, 4959 + [O II] λ3726, 3729)/Hβ (hereinafter O_{23}) (Pagel et al. 1979; McGaugh 1991) at the isophotal radius, interpolated from the values observed in giant H II regions. In other contexts, however, it has been suggested that the extinction derived from the Balmer decrement might be related to metallicity. For example, Campbell et al. (1986) found a loose correlation between the extinction and the oxygen abundance in a sample of H II galaxies. Also, invidivual giant H II regions in spiral galaxies exhibit a decrease of extinction with galactocentric radius (Kennicutt & Garnett 1996; Van Zee et al. 1998a), but this is not a general rule (Martin & Roy 1992 and references therein).

Figure 3 shows $C_{\rm l}$ as a function of the usual metallicity indicator O_{23}. The meaning of the symbols is the same as in Fig. 2. When considering only the filled symbols, there is a weak correlation in the sense that O_{23} tends to be smaller for larger values of $C_{\rm l}$. The correlation virtually disappears when including the open symbols, for which the extinction and reddening corrected line ratios tend to be more uncertain. These results are confirmed by Kendall's τ statistical test; see Table 1. We know that the relation between O_{23} and O/H is double valued, with a maximum in O_{23} occuring at log O/H + 12 of about 8.2. This is illustrated in Fig. 4, which shows O_{23} versus O/H as computed for a sequence of simple constant density models roughly representative of giant H II regions, using the photoionization code PHOTO described in Stasińska & Leitherer (1996). Because radial abundance gradients are known to exist in spiral galaxies from the study of their bright giant H II regions (Vilas-Costas & Edmunds 1992; Zaritsky et al. 1994), it is conceivable that, depending on the abundance gradients and the relative weights of the regions of various abundances in the integrated emission line fluxes, O_{23} might not be a a good indicator of the galaxy overall metallicity. It is important to note that metallicity here refers only to the star formation regions. Kobulnicky et al. (1999) have addressed this problem by simulating the global O_{23} of 22 spiral galaxies, integrating the observed values for several bright individual H II regions over the Hα radial profiles from CCD images. They found that the oxygen abundance derived from the

Table 1. Results of Kendall's τ non parametric test for the observational diagrams.

figure number	whole sample			sample with $EW(\mathrm{H}\beta) > 5$ Å and $EW(\mathrm{H}\alpha) > 10$ Å		
	N	τ	*prob*	N	τ	*prob*
1	110	8.79E-01	3.69E-42	70	7.93E-01	2.66E-22
2	104	6.69E-01	8.05E-24	66	6.28E-01	8.77E-14
3	104	−2.24E-01	7.71E-04	66	−4.20E-01	6.00E-07
6	104	6.00E-01	1.69E-19	66	6.01E-01	9.90E-13
7	104	4.09E-01	7.37E-10	66	5.34E-01	2.23E-10
8a	116	−5.50E-01	2.06E-18	70	−2.53E-01	1.96E-03
8b	123	−5.27E-01	5.74E-18	70	−2.40E-01	3.31E-03
8c	81	−5.24E-01	4.40E-12	64	−4.99E-01	5.65E-09
8d	116	−2.34E-02	7.09E-01	68	4.24E-01	3.19E-07
9a	116	3.40E-01	6.28E-08	70	5.31E-03	9.48E-01
9b	123	3.44E-01	1.72E-08	70	1.09E-01	1.81E-01
9c	81	2.29E-01	2.44E-03	64	1.68E-01	5.02E-02
9d	116	−2.23E-03	9.72E-01	68	−3.75E-01	5.96E-06
10a	94	−4.78E-01	8.70E-12	70	−5.20E-01	1.87E-10
10b	94	2.63E-01	1.75E-04	70	2.44E-01	2.85E-03
10c	108	4.37E-01	2.12E-11	70	5.83E-01	9.54E-13
10d	106	6.36E-01	4.19E-22	68	6.32E-01	2.61E-14
11a	108	−5.38E-01	1.49E-16	70	−5.87E-01	6.47E-13
11b	108	−5.03E-01	1.15E-14	70	−5.38E-01	4.34E-11
11c	108	3.36E-01	2.53E-07	70	3.84E-01	2.66E-06

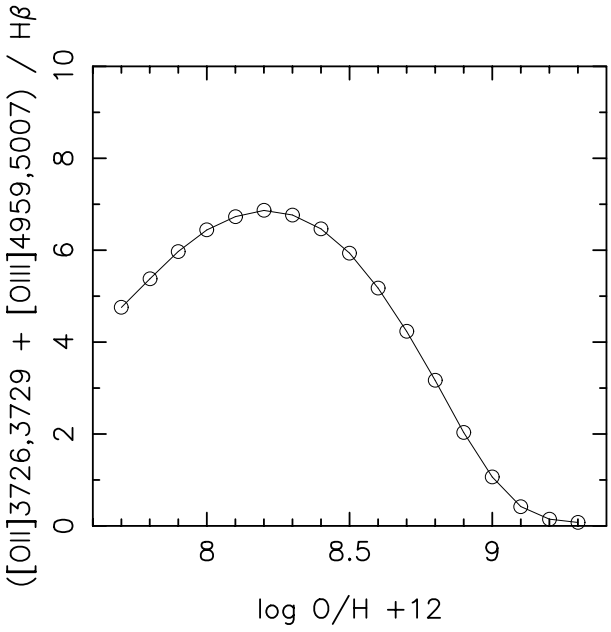

Fig. 4. [O III] λ5007, 4959 + [O II] λ3726, 3729)/Hβ as a function of O/H for a series of photoionization models representative of giant H II regions (total number of ionizing photons 3×10^{51} ph s^{-1}, effective temperature 45 000 K, density 100 cm^{-3} and filling factor 0.03).

simulated integrated O_{23} was identical, within errors, to the characteristic abundance of galaxies defined by Zaritsky et al. (1994) as the oxygen abundance computed at a certain characteristic galactocentric radius. They concluded that the beam smearing effect from sampling large number of galaxies, even in the presence of strong abundance gradients, has a small effect on characterizing the mean abundances of galaxies. They mention however, that it would be useful to test this conclusion directly using actual integrated spectra of galaxies. Unfortunately, none of the galaxies in their sample belongs to the NFGS sample. Our conclusion using the NFGS sample is purely empirical, and is that O_{23} does not seem to be a useful indicator of metallicity in integrated spectra.

Another indirect empirical metallicity indicator has been proposed more recently (van Zee et al. 1998a), which has the double advantage of not being plagued by the double value problem and of being independent of reddening. This is the [N II] λ6584/Hα ratio. Figure 5, obtained from the same models as Fig. 4 (these models assume that N/O α $(\mathrm{O/H})^{0.5}$) shows that [N II] λ6584/Hα increases with O/H up to log O/H + 12 around 8.8. There are two reasons for such a behaviour. One is that [N II] λ6584/Hα is less dependent on the electron temperature than O_{23}, so that it is not so much affected by the decrease in electron temperature provoked by an increase in metallicity. The other reason is that N/H increases with O/H. The study of giant H II regions in spiral galaxies (van Zee et al. 1998b) indicates that at log O/H + 12 > 8.5, N/O is proportional to O/H and not to $(\mathrm{O/H})^{0.5}$, so that the effect is even stronger than in the models shown in Fig. 5.

Figure 6 shows C_1 as a function of [N II] λ6584/Hα for the normal galaxies in the NFGS sample. There is a very clear correlation! Kendall's τ is 0.6 and the small

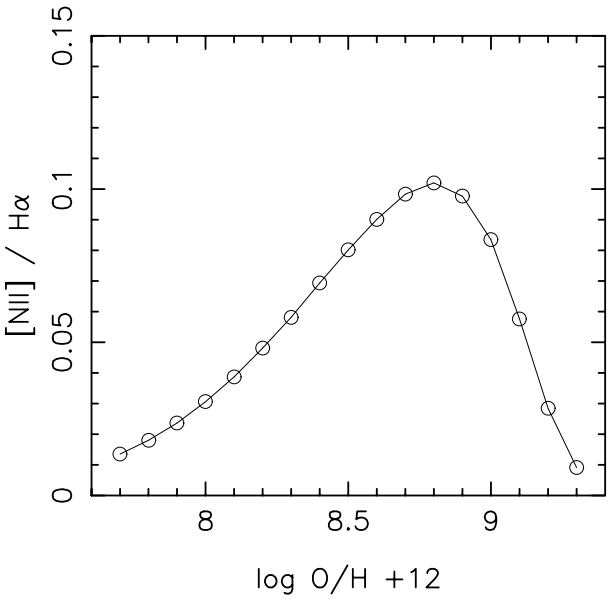

Fig. 5. Same as Fig. 4, but for [N II] λ6584/Hα.

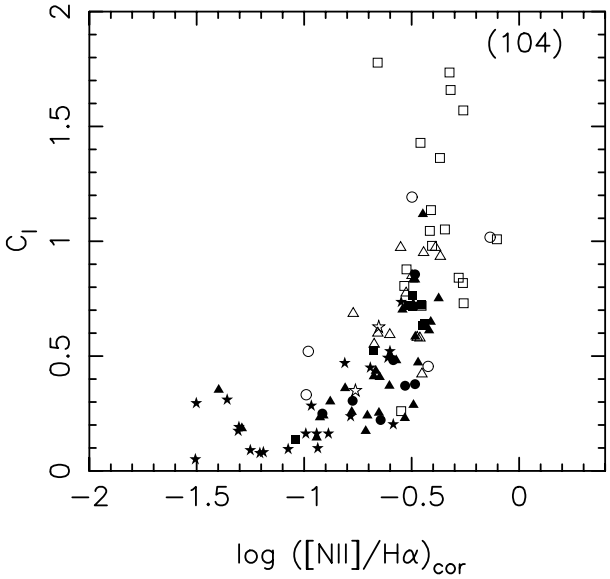

Fig. 6. C_l as a function of [N II] λ6584/Hα corrected for reddening. Same symbols as in Fig. 2.

value of *prob* indicates that the correlation is highly significant. As a matter of fact, it is even surprising that such a good correlation should exist. Indeed, the [N II] λ6584/Hα ratio obviously strongly depends on the ionization parameter of the H II regions. While giant H II regions seem to follow a very narrow sequence in ionization parameters (McCall et al. 1985; Dopita & Evans 1986; Stasińska et al. 2001), one expects in integrated spectra of spiral galaxies a non negligible contribution from a diffuse medium, possibly ionized by photons leaking out of bona fide giant H II regions. Indeed, about 20 to 50% of the H-Balmer line emission in nearby spiral galaxies arises from this diffuse medium (e.g., Greenawalt et al. 1997; Collins et al. 2000; Rossa & Dettmar 2000; Zurita et al. 2000;

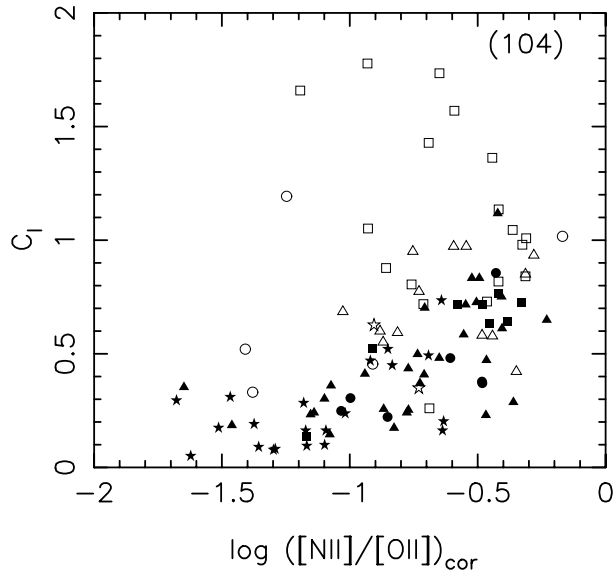

Fig. 7. C_l as a function of [N II] λ6584/[O II] λ3727 corrected for reddening. Same symbols as in Fig. 2.

Rand 2000). The [N II] λ6584/Hα ratios observed in this diffuse medium are typically a factor 2 larger than in the nearby giant H II regions, which implies that in an integrated spectrum, the effect of the diffuse medium at a given galactocentric distance (and therefore metallicity) is to increase the [N II] λ6584/Hα ratio by about 30% at most. Such an increment is relatively modest compared to the metallicity dependence of this ratio and explains why [N II] λ6584/Hα appears to be such a good indicator of the overall metallicity of spiral galaxies. We should emphasize that, nevertheless, this indicator cannot be easily translated into a value of O/H, in the presence of abundance gradients and integration over the complex interstellar medium of spiral galaxies. For example, the weight of the regions of metallicities around solar is expected to be important, as seen from Fig. 5. One should certainly refrain from using the calibration that has been proposed by van Zee et al. (1998a), which is valid only in the context of giant H II regions.

Another potential empirical indicator of metallicity of the emission line regions which is independent of the ionization parameter, does not suffer from the double value problem and is less affected by metallicity gradients is [N II] λ6584/[O II] λ3727 (Dopita et al. 2000). It is however strongly dependent on the reddening correction. Figure 7 shows C_l as a function of [N II] λ6584/[O II] λ3727 (the open symbols have the same meaning as in Figs. 2, 3 and 6), and here again we clearly see a correlation. It is more dispersed than the C_l versus [N II] λ6584/Hα relation, possibly because of errors in the reddening correction. Indeed, the correlation is much better when considering only the filled symbols. This is confirmed by the results of Kendall's τ test presented in Table 1.

From the above considerations, our conclusion is that, indeed, C_l correlates with the global metallicity of the emission line regions in spiral galaxies, at variance with the

conclusions of Zaritsky et al. (1994). It should be stressed that $C_{\rm l}$ does not necessarily measure the true extinction of the total light emitted in the Balmer lines. In the case of a patchy dust distribution, it measures, so to say, the effective extinction of those regions that are not too strongly obscured, so that the interpretation of our result is by no means straightforward.

3. The emission line sequence

In SS99, we showed that, when ordering the normal galaxies from the Kennicutt sample by galaxy spectral type, emission line equivalent widths and emission line ratios from the integrated galaxy spectra formed a very well defined sequence (not necessarily monotonic!). We interpreted this as evidence for a close link between the high mass end of the stellar populations, which drive the emission lines, and the population of the stars that are responsible for the optical continuum, which determines the galaxy spectral type. The scatter in the properties of individual H II regions observed in spiral galaxies (Kennicutt & Garnett 1996; Roy & Walsh 1997) is likely to be smoothed out in integrated galaxy spectra if the galaxies are sufficiently massive to contain a large number of H II regions. The sequence found by SS99 was so impressive, that it calls for further investigation and the NFGS sample is adequately large for such a purpose. Unfortunately, we cannot determine the galaxy spectral type from the published data, since the spectra are not yet publicly available in digital form. As a proxy of the galaxy spectral type, we can use galaxy colours, with the advantage that they are much easier to obtain than spectral types. We found empirically that the best colour to use was the synthetic $(B-R)$ derived from the galaxy spectra as explained by Jansen et al. (2000b).

3.1. Equivalent widths and star formation

In Fig. 8, we show the equivalent widths of Hα, [O II] λ3727, [O III] λ5007 and [N II] λ6584 as a function of $(B-R)$. The shape of the symbols represent the galaxy morphological types, as in the previous observational diagrams. Clearly, the equivalent widths of Hα, [O II] λ3727 and [O III] λ5007 are strongly correlated with $(B-R)$, being larger for bluer galaxies. However, there seems to be more dispersion than was suggested by the study of SS99. One possible reason is that the color $(B-R)$ is not as good a parameter as the spectral type for ranking galaxies. For comparison, we show in Fig. 9 the same equivalent widths but as a function of the galaxy morphological type, T. The correlations of equivalent widths with T are seen to be much weaker than with $(B-R)$. These conclusions are confirmed by the statistical test summarized in Table 1.

Emission lines, principally Hα and [O II] λ3727, are indicators of current star formation (Barbaro & Poggianti 1997; Kennicutt 1998; Jansen et al. 2001). The calibration in terms of star formation rates however strongly depends on several factors: star formation law, metallicity, selective dust extinction, etc. Charlot & Longhetti (2001) argue for the necessity of using the [O II] λ3727, [O III] λ5007 Hα and Hβ lines at the same time to better constrain the problem. Qualitatively, though, Fig. 8 (together with Fig. 1) shows that any of these parameters is likely to be a first order ranking indicator of integrated star formation rates in spiral galaxies. This is of course not the case of [N II] λ6584, whose equivalent width behaves in a completely different manner. Indeed, the strong drop in nitrogen abundance for the bluest (less chemically evolved) galaxies overtakes the effects of increasing present star formation rate and increasing electron temperature.

As shown by Jansen et al. (2000b), equivalent widths are also loosely correlated with galaxy absolute magnitudes, tending to be larger for more luminous galaxies. However, at a given galaxy colour, we found no compelling evidence of brighter galaxies having larger equivalent widths.

3.2. Line ratios and metallicity

Figure 10 shows various emission line ratios as a function of $(B-R)$. The line ratios have been dereddened using the value of C_l computed above. Since the reddening correction becomes more uncertain for galaxies with small $EW(\mathrm{H}\alpha)$ and $EW(\mathrm{H}\beta)$, as in Figs. 2, 3, 6 and 7 we marked by filled symbols those objects that have $EW(\mathrm{H}\alpha) > 10$ Å and $EW(\mathrm{H}\beta) > 5$ Å and thus the most reliable reddening corrections. Clear trends are seen for [O III] λ5007/[O II] λ3727, [N II] λ6584/[O II] λ3727 and [N II] λ6584/Hα as a function of $(B-R)$. As for the equivalent widths, we find the trends much clearer with $(B-R)$ than with morphological type. For [O III] λ5007/[O II] λ3727 and [N II] λ6584/[O II] λ3727, which are sensitive to reddening, one can see that the open symbols prolong the trends defined by the filled symbols, but with much higher dispersion. In the case of O_{23}, there is a weak trend with $(B-R)$ when considering only the filled symbols, and practically no trend when considering the entire data set. The statistical significance of these trends are presented in Table 1.

The fact that [O III] λ5007/[O II] λ3727 decreases as the galaxy color gets redder is not necessarily only due to a lowering of the average ionization parameter or the average spectral hardness of the exciting stars (as was suggested by SS99). Indeed, an increase in overall metallicity, by enhancing the temperature drop in the central zones of H II regions with metallicities larger than solar, also contributes to lower the [O III] λ5007/[O II] λ3727 ratio (see Stasińska et al. 2001). We find no trend of [S II]/Hα with colour, suggesting that the effect of ionization parameter along the colour sequence may not be overwhelming.

As mentioned in Sect. 2, the O_{23} ratio is not the best indicator of metallicity in integrated spectra of galaxies where abundance gradients are known to occur. Being non monotonic with respect to the metallicities of individual H II regions, when integrated over an entire galaxy it becomes impossible to interpret without additional

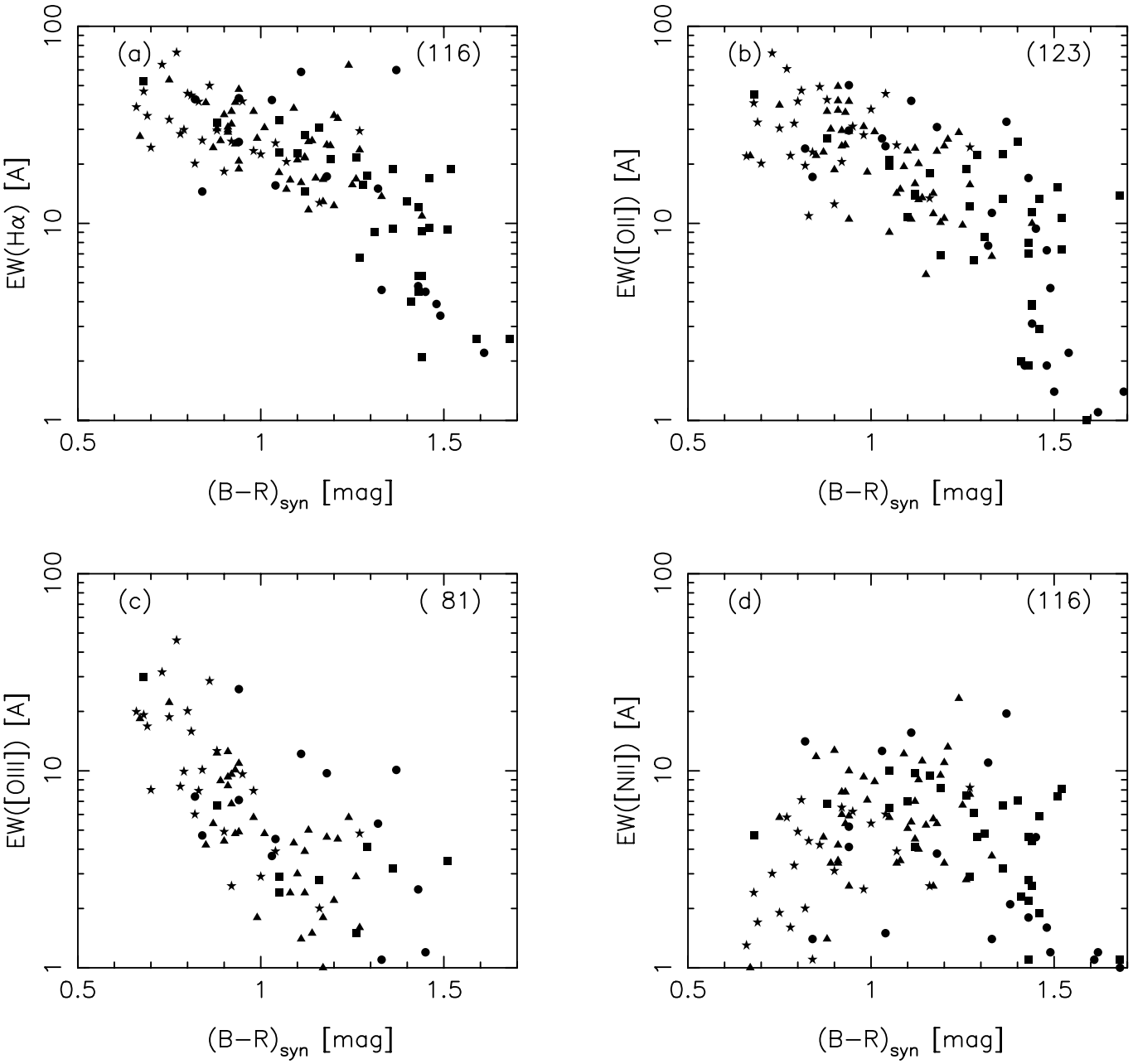

Fig. 8. Emission line equivalent widths as a function of the galaxy colour $(B-R)$. **a)** Hα; **b)** [O II] λ3727; **c)** [O III] λ5007; **d)** [N II] λ6584. Same symbols as in Fig. 1.

information on the radial galactic gradients in abundances and star formation rates. In addition, it is strongly dependent on the reddening correction, which becomes uncertain in metal rich galaxies with weak lines.

On the other hand, [N II] λ6584/[O II] λ3727 is a good indirect indicator of metallicity in extragalactic H II regions (Dopita et al. 2000) and is expected to be a fair indicator of overall metallicity in integrated galaxy spectra (see above). The trend seen in Fig. 10c is produced by an increase of N/O as galaxy colour gets redder, indirectly indicating an increase in metallicity. As a consequence, the conspicuous trend of [N II] λ6584/Hα increasing with $(B-R)$ (Fig. 10d), is likely due to an increase in metallicity. As mentioned before, the [N II] λ6584/Hα ratio has the advantage of being reddening-independent, and it can be used with confidence even for galaxies with weak emission lines. It clearly indicates that the sequence between metallicity and $(B-R)$ colour is quite narrow even for galaxies redder than $(B-R)=1.2$ (which is not apparent when using the strongly reddening-dependent [N II] λ6584/[O II] λ3727 ratio).

Numerous studies have claimed the existence of a metallicity-luminosity relation in a variety of classes of galaxies: dynamically hot galaxies, i.e. ellipticals, bulges, and dwarf spheroidals, dwarf H II galaxies, irregular galaxies and spirals (Bender et al. 1993; Vigroux et al. 1987;

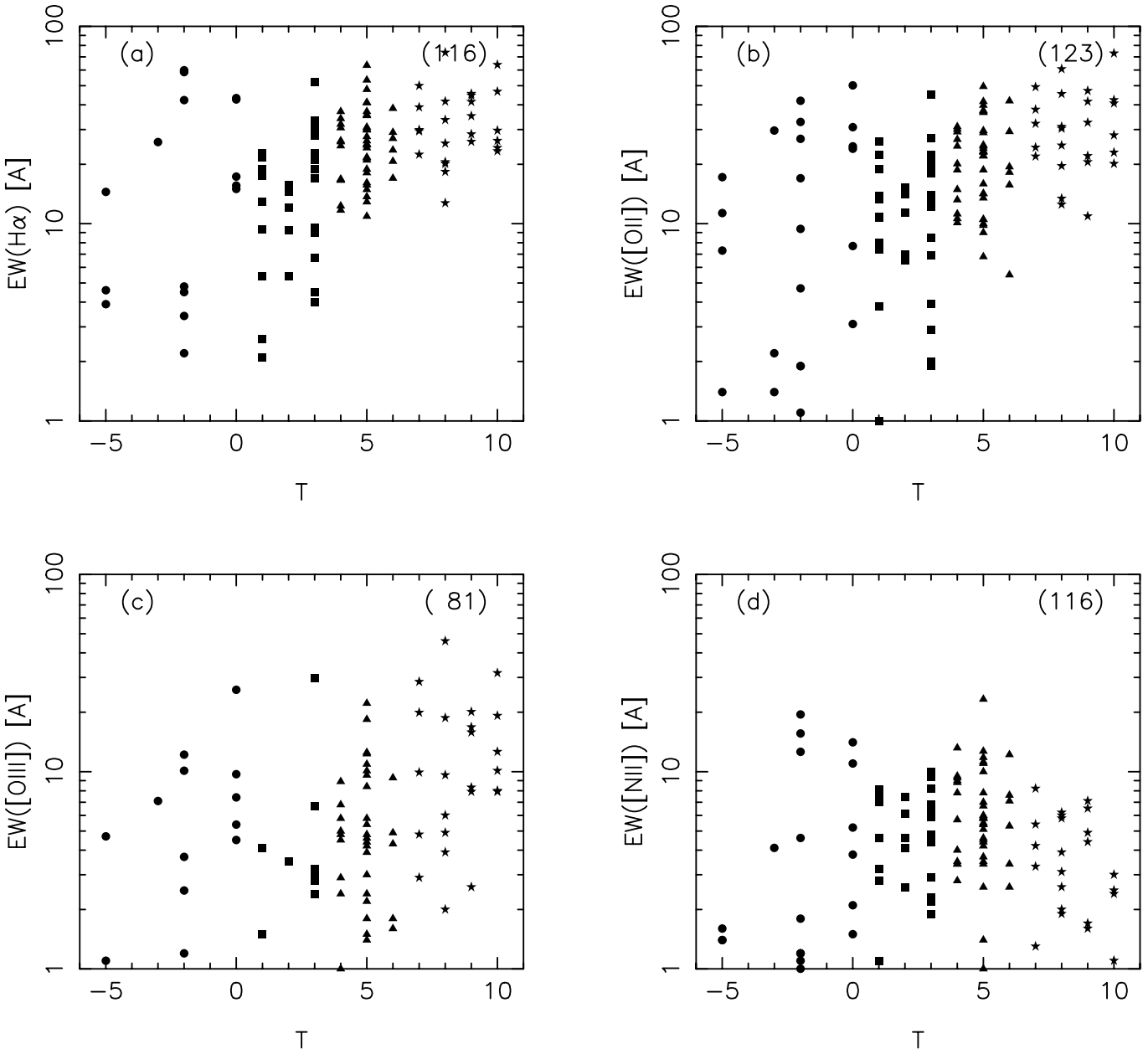

Fig. 9. Emission line equivalent widths as a function of the galaxy morphological type T. **a)** Hα; **b)** [O II] λ3727; **c)** [O III] λ5007; **d)** [N II] λ6584. Same symbols as in Fig. 1.

Skillman et al. 1989; Richer & McCall 1995; Zaritsky et al. 1994). In Fig. 11, we show the various metallicity indexes, O_{23}, [N II] λ6584/Hα and [N II] λ6584/[O II] λ3727 as a function of the total absolute blue magnitude M_B. We do find a strong correlation between M_B and the metallicity indexes [N II] λ6584/Hα and [N II] λ6584/[O II] λ3727. The correlation of the O_{23} index with M_B is statistically significant (see Table 1), but at a rather low level. It is interesting to recall that Zaritsky et al. (1994), by using this index to infer the characteristic metallicity of spiral galaxies, did find a trend with galaxy luminosity. But the index actually referred to the observed ratio at a certain galactic radius, and not to the integrated light from the galaxy. Our study has shown how misleading the use of O_{23} can be in integrated spectra of galaxies in the presence of abundance gradients. On the other hand, [N II] λ6584/Hα and [N II] λ6584/[O II] λ3727 show clear trends with galaxy absolute magnitude, confirming that indeed, there is a relation in spiral galaxies between the overall metallicity of the star forming regions and the galaxy luminosity.

4. Principal component analysis

Principal Component Analysis (PCA) is a useful tool for the examination of multidimensional data and the identification of underlying variables that may be responsible for the variance in a data set (Murtagh & Heck 1987; Fukunaga 1990). PCA allows one to define a new

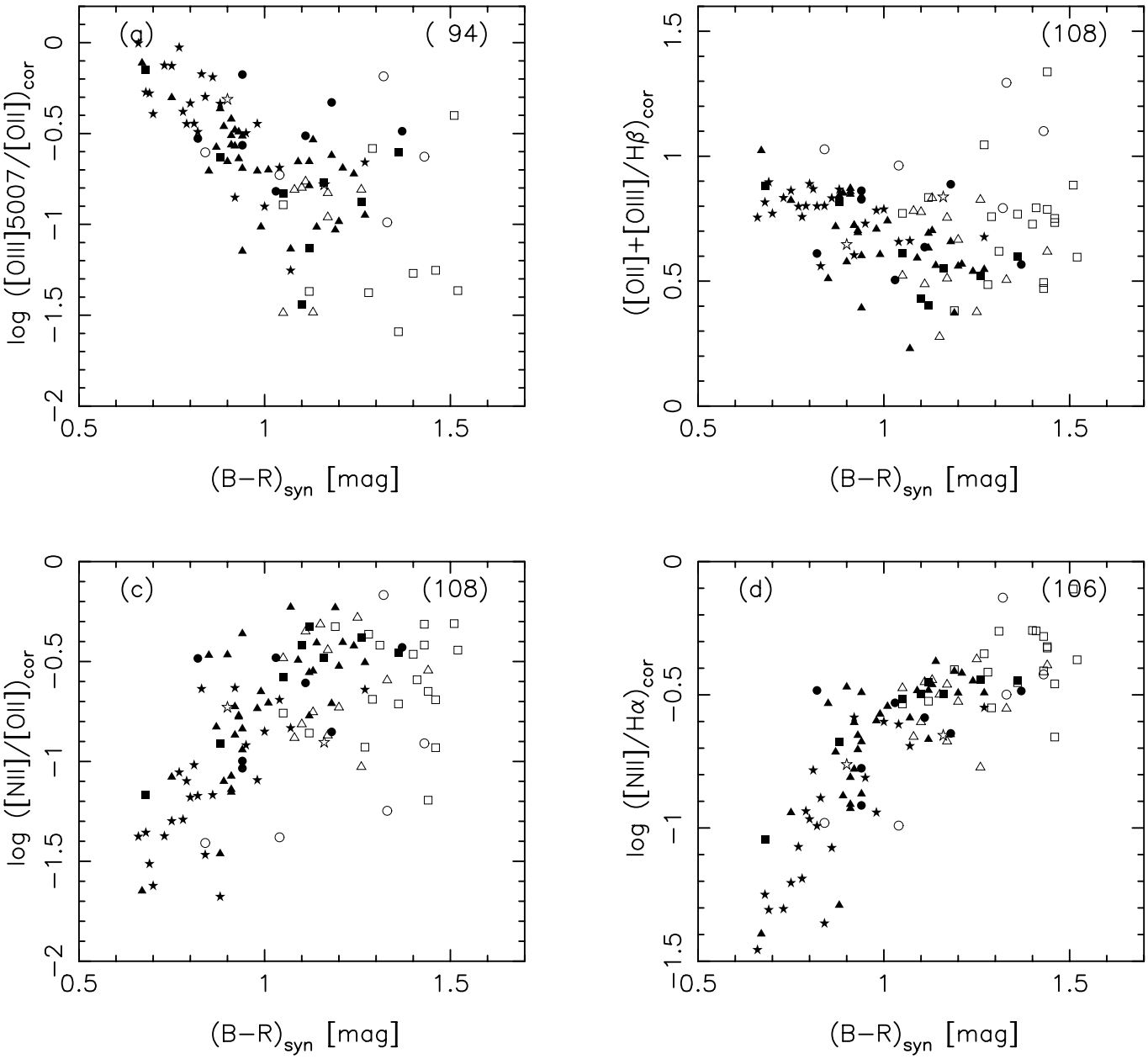

Fig. 10. Emission line ratios corrected for reddening as a function of the galaxy colour ($B-R$). **a)** [O III] λ5007/[O II] λ3727; **b)** ([O III]+ [O II])/Hβ; **c)** [N II] λ6584/[O II] λ3727; **d)** [N II] λ6584/Hα. Same symbols as in Fig. 2.

orthonormal reference system in a parameter space, with basis-vectors (the principal components) spanning directions of maximum variance.

Here we apply PCA to a set of variables describing different aspects of the galaxies in the NFGS sample. The 7 variables selected for this exercise are: the blue absolute magnitude M_B; the color $(B-R)$; the numerical value of the morphological type T; the galaxy surface brightness at the effective radius $\mu_B^{\rm e}$; $EW(\rm H\alpha)$, which is related to the star formation rate; the metallicity indicator [N II] λ6584/Hα; and Hα/Hβ, related to the emission-line extinction. The number of normal galaxies with complete information that enters in the analysis is 102.

Since the input variables are of different natures, it is appropriate to apply PCA on the correlation matrix, that is, the input variables were transformed: they had their mean value subtracted and, after, they were divided by their standard deviation. Hence the analysis is made on a set of transformed variables with zero mean and unity variance. The result indicates that the first principal component alone explains 48% of the sample variance. The second and third components are responsible for 19% and 12% of the sample variance, respectively.

Although each principal component is a linear combination of all the input variables, it is interesting to verify whether some variables are well correlated with the first components because, in this case, they are responsible for

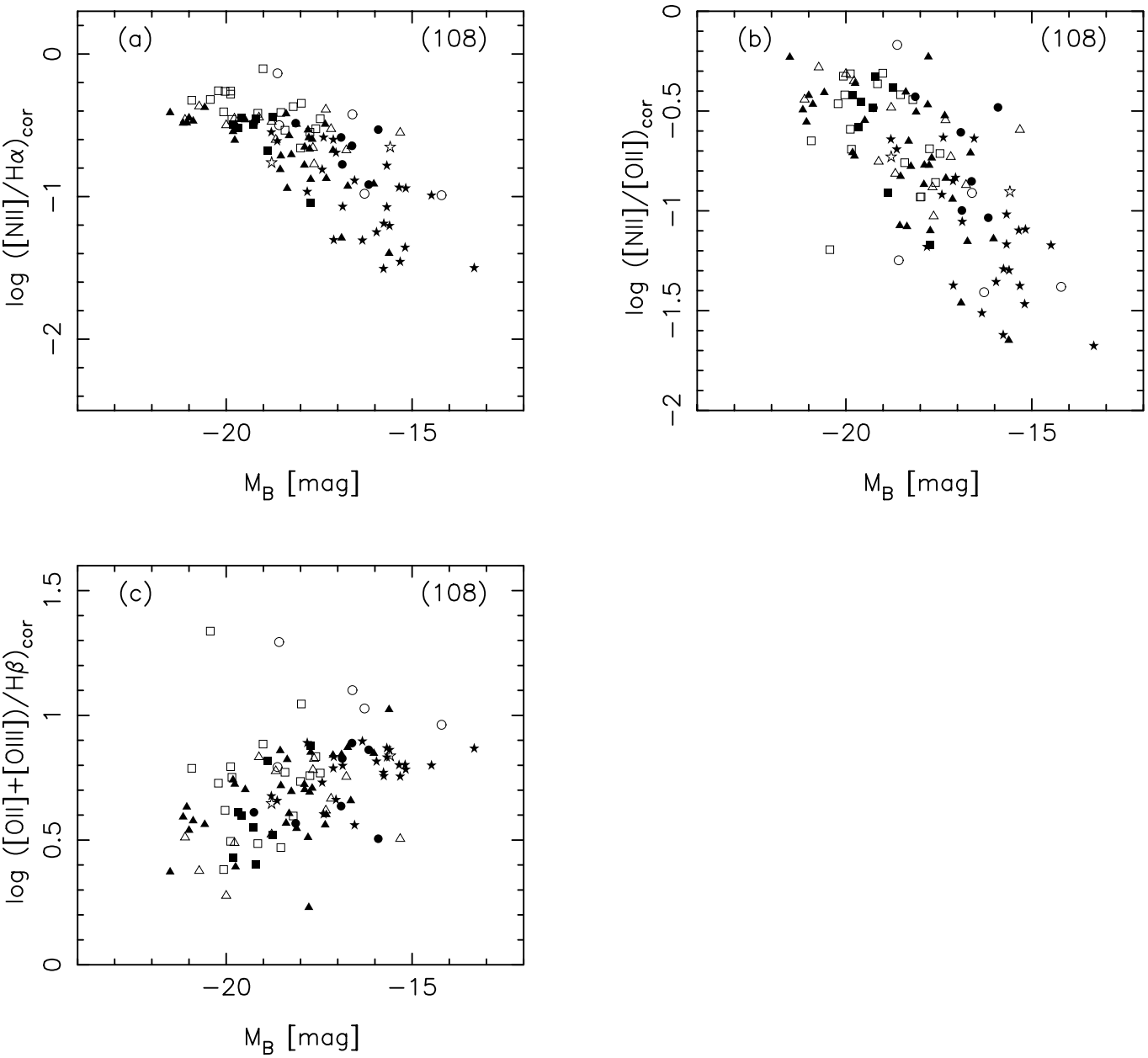

Fig. 11. Emission line ratios corrected for reddening as a function of the galaxy absolute blue magnitude M_B. **a)** [N II] λ6584/Hα; **b)** [N II] λ6584/[O II] λ3727; **c)** ([O III]+ [O II])/Hβ. Same symbols as in Fig. 2.

a significant fraction of the sample variance. We have then computed, for each variable and principal component, the non-parametric Kendall's τ coefficient of rank correlation and the respective probability of absence of correlation between these quantities. We found that the variable that best correlates with the first component is the metallicity indicator [N II] λ6584/Hα; the variables $(B-R)$, and Hα/Hβ also correlate well with the first component; the morphological type is correlated with the first principal component, but to a lesser extent. On the other side, only μ_B^e is strongly correlated with the second principal component. The absolute magnitude correlates best with the third principal component. Hence, this analysis indicates that the variance in the parameter space considered here is produced, in first place, by the metallicity and parameters related to it or to the stellar populations, and, in second place, by the surface brightness, which is related to the dynamical history of the galaxies. The absolute magnitude, related to the mass of the galaxy, surprisingly comes only in third place.

5. Conclusions

We have explored the emission line trends from the integrated spectra of normal spiral galaxies, in order to investigate the relationships between dust extinction, metallicity and some macroscopic properties of spiral galaxies.

A similar aim was followed by the study by Zaritsky et al. (1994) on a sample of 39 disk galaxies, which however was not based on integrated spectra of galaxies, but on the study of several giant H II regions in each galaxy. Our approach, using integrated spectra, is a priori likely to give more robust answers. It also has the advantage of being readily applicable to studies of galaxies at high redshift. We benefited from data from the Nearby Field Galaxy Survey (Jansen et al. 2000a, b), which considerably increased the size of the so far available samples for systematic studies of the global properties of spiral galaxies.

Our main results are the following.

We found that the correlation between $EW(\mathrm{H}\alpha)$ and $EW(\mathrm{H}\beta)$ is extremely strong. This implies that $C_\mathrm{l} - C_\mathrm{c}$, the difference between the effective extinction of the stellar and the nebular light, depends only on the intrinsic colours of the galaxies, being larger for redder galaxies.

The nebular extinction as derived from the Balmer decrement is found to correlate essentially with the effective metallicity of the emission line regions. This finding required using an appropriate metallicity indicator. The usual O_{23} index does not work for integrated spectra of galaxies, due to strong metallicity gradients. On the other hand, [N II] λ6584/Hα and [N II] λ6584/[O II] λ3727 seem to be adequate empirical metallicity indicators, the first one having the advantage of being reddening-independent and being applicable also to galaxies with weak emission lines. The calibration of these indicators would require a modelling of the integrated spectra of galaxies, in the vein of the works of Charlot & Longhetti (2001) or Moy et al. (2001) but including the effects of radial gradients in the metallicity and star formation rates.

We find that the overall metallicity of the emission line regions, as inferred from adequate indicators, is strongly correlated with galaxy colours. The correlation is much stronger than with morphological types. This suggests that in normal spiral galaxies, the global metallicity of the star-forming regions and the old stellar populations are closely linked, while morphological types are influenced by additional factors in the galaxy histories.

In order to better evaluate the relation between the different parameters describing the galaxies, we performed a PCA analysis on a 7-D parameter space. We found that the variance in the considered parameter space is produced, in first place, by the metallicity and parameters linked to the stellar populations, and, in second place, by the surface brightness, which is linked to the dynamical history of the galaxies. The absolute magnitude, related to the mass of the galaxy, comes only in third place.

The strong empirical evidence provided by this exploratory work bring important constraints that will have to be reproduced by models of spiral galaxy formation and evolution, in order to understand what drives the spiral galaxy sequence.

Acknowledgements. This study would not have been possible without the huge observational work by R. A. Jansen, D. Fabricant, M. Franx & N. Caldwell, and we acknowledge these authors for having made available their results on the Web. We benefited from financial help from CNRS and CNPq. G. S. warmly acknowledges the IAG and L. S. the DAEC for hospitality. L. S. also acknowledges Fapesp and Pronex for support.

References

Balogh, M. L., Morris, S. L., Yee, H. K. C., Carlberg, R. G., & Ellingson, E. 1999, ApJ, 527, 54
Barbaro, G., & Poggianti, B. M. 1997, A&A, 324, 490
Bender, R., Burstein, D., & Faber, S. M. 1992, ApJ, 399, 46
Caldwell, N., Rose, J. A., Sharpless, R. M., Ellis, R. S., & Bower, R. G. 1993, AJ, 106, 473
Calzetti, D., Kinney, A. L., & Storchi-Bergmann, T. 1994, ApJ, 429, 582
Calzetti, D., Kinney, A. L., & Storchi-Bergmann, T. 1996, ApJ, 458, 132
Calzetti, D. 1997, AJ, 113, 162
Campbell, A., Terlevich, R., & Melnick, J. 1986, MNRAS, 223, 811
Charlot, S., & Fall, S. M. 2000, ApJ, 539, 718
Charlot, S., & Longhetti, M. 2001, MNRAS, 323, 887
Cid Fernandes, R., Sodré, L., Schmitt, H. R., & Leão, J. R. S. 2001, MNRAS, in press
Colless, M., Ellis, R. S., Taylor, K., & Hook, R. N. 1990, MNRAS, 244, 408
Collins, J. A., Rand, R. J., Duric, N., & Walterbos, R. A. M. 2000, ApJ, 536, 645
Connolly, A. J., Szalay, A. S., Bershady, M. A., Kinney, A. L., & Calzetti, D. 1995, AJ, 110, 1071
de Vaucouleurs, G. 1959, AJ, 64, 397
Disney, M., Davies, J., & Phillipps, S. 1989, MNRAS, 239, 939
Dopita, M. A., & Evans, I. N. 1986, ApJ, 307, 431
Dopita, M. A., Kewley, L. J., Heisler, C. A., & Sutherland, R. S. 2000, ApJ, 542, 224
Dressler, A., Smail, I., Poggianti, B., et al. 1999, ApJS, 122, 51
Fanelli, M. N., O'Connell, R. W., & Thuan, T. X. 1988, ApJ, 334, 665
Fioc, M., & Rocca-Volmerange, B. 1997, A&A, 326, 950
Folkes, S. R., Lahav, O., & Maddox, S. J. 1996, MNRAS, 283, 651
Fukunaga, K. 1990, Statistical Pattern Recognition (Academic Press, New York)
Galaz, G., & de Lapparent, V. 1998, A&A, 332, 459
Giovanelli, R., Haynes, M. P., Salzer, J. J., et al. 1994, AJ, 107, 2036
Greenawalt, B., Walterbos, R. A. M., & Braun, R. 1997, ApJ, 483, 666
Guzman, R., Koo, D. C., Faber, S. M., et al. 1998, ApJ, 460, L5
Hammer, F., Flores, H., Lilly, S. J., et al. 1997, ApJ, 481, 49
Holmberg, E. 1958, Medd. Lunds Astr. Obs. Ser., 2, No. 136
Holmberg, E. 1975, in Stars and Stellar Systems, vol. IX, ed. A. Sandage, M. Sandage, & J. Kristian (University of Chicago Press, Chicago), Chap. 4, 123
Isobe, T., Feigelson, E. D., Akritas, M. G., & Babu, G. J. 1990, ApJ, 364, 104
James, P. A., & Puxley, P. J. 1993, Nature, 363, 240
Jansen, R. A., Franx, M., Fabrikant, D., & Caldwell, N. 2000a, ApJS, 126, 271

Jansen, R. A., Fabrikant, D., Franx, M., & Caldwell, N. 2000b, ApJS, 126, 331
Jansen, R. A., Franx, M., & Fabrikant, D. 2001, ApJ, 551, 825
Kennicutt, R. C. 1992, ApJS, 79, 255
Kennicutt, R. C., & Garnett, D. R. 1996, ApJ, 456, 504
Kennicutt, R. C. 1998, ARA&A, 36, 189
Kobulnicky, H. A., Kennicutt, R. C., & Pizagno, J. L. 1999, ApJ, 514, 544
Lilly, S., Schade, D., Ellis, R. S., et al. 1998, ApJ, 500, L75
Maíz-Apellániz, J., Mas-Hesse, J. M., Muñoz-Tuñon, C., Vílchez, J. M., & Castañeda, H. O. 1998, A&A, 329, 409
Martin, P., & Roy, J. R. 1992, ApJ, 397, 463
Mayya, Y. D., & Prahbu, T. P. 1996, AJ, 111, 1252
McCall, M. L., Rybski, P. M., & Shields, G. A. 1985, ApJS, 57, 1
McGaugh, S. S. 1991, ApJ, 380, 140
Meurer, G. R., & Seibert, M. 2001 [astro-ph/0101479]
Morgan, W. W., & Mayall, N. U. 1957, PASP, 69, 291
Moy, E., Rocca-Volmerange, B., & Fioc, M. 2001, A&A, 365, 347
Murtagh, F., & Heck, A. 1987, Multivariate Data Analysis (Reidel, Dordrecht)
Nelson, A. E., Zaritsky, D., & Cutri, R. M. 1998, AJ, 115, 2273
Pagel, B. E. J., Edmunds, M. G., Blackwell, D. A., Chun, M. S., & Smith, G. 1979, MNRAS, 189, 95
Peletier, R. F., Valentijn, E. A., Moorwood, A. F. M., et al. 1995, A&A, 300, L1
Poggianti, B., Smail, I., Dressler, A., et al. 1999, ApJ, 518, 576
Poggianti, B., & Wu, H. 2000, ApJ, 529, 157
Press, W. H., Teukolsky, S. A., Vetterling, W. T., & Flannery, B. P. 1992, Numerical Recipes (Cambridge University Press)
Rand, R. J. 2000, ApJ, 537, L13
Richer, M. G., & McCall, M. L. 1995, ApJ, 449, 642
Rossa, J., & Dettmar, R.-J. 2000, A&A, 359, 433
Roy, J. R., & Walsh, J. R. 1997, MNRAS, 288, 715 U
Seaton, M. J. 1979, MNRAS, 187, 73
Skillman, E. D., Kennicutt, R. C., & Hodge, P. W. 1989, ApJ, 347, 875
Sodré, L., & Cuevas, H. 1994, Vistas Astron., 38, 287
Sodré, L., & Cuevas, H. 1997, MNRAS, 287, 137
Sodré, L., & Stasińska, G. 1999, A&A, 345, 391
Stasińska, G., & Leitherer, C. 1996, ApJS, 107, 661
Stasińska, G., Schaerer, D., & Leitherer, C. 2001, A&A, 370, 1
Valentijn, E. A. 1990, Nature, 346, 153
van Zee, L., Salzer, J. J., Haynes, M. P., O'Donoghue, A. A., & Balonek, T. J. 1998a, AJ, 116, 2805
van Zee, L., Salzer, J. J., & Haynes, M. P. 1998b, ApJ, 497, L1
Vigroux, L., Stasińska, G., & Comte, G. 1987, A&A, 172, 15
Vilas-Costas, M. B., Edmunds, & M. G. 1992, MNRAS, 259, 121
Wang, B., & Heckman, T. M. 1996, ApJ, 457, 645
Witt, A. N., Thronson, H. A., & Capuano, J. M. 1992, ApJ, 393, 611
Zaritsky, D., Kennicutt, R. C., & Huchra, J. P. 1994, ApJ, 420, 87
Zurita, A., Rozas, M., & Beckman, J. E. 2000, A&A, 363, 9